

4.0 DETAILED DESCRIPTION OF TECHNICAL PROGRESS

4.1 Task A - Rates of Carbon Formation

4.1.1 Experimental Equipment

During the first few months of the program, the multiple fixed-bed reactor system designed and constructed under DOE Contract No. EX-76-C-01-2036 was refurbished and modified. This system is depicted in Figures 4 and 5 along with the control panel and booster compressor diagrams in Figures 6 and 7, respectively. Modifications to the system include - high/low temperature and pressure alarm systems - capillary tube water injector to prevent pulse feeding of steam - and a regeneration gas mixing station.

The reactor design incorporates a removable multi-section catalyst basket which can be positioned inside the reactor pipe. In each of the baskets, a provision is provided to allow for a central thermowell. Contained inside the thermowell are three traveling thermocouples used in obtaining the temperature profile along the catalyst bed.

The tubular reactor consists of a three (3) foot long 316 SS, one inch Schedule 80 pipe with a male weld connection welded to each end. Feed gas enters the top of the reactor through 1/4" SS tubing. Water, when utilized, is injected into this 1/4" tubing through 1/16" SS capillary tubing. The feed gas then passes through a 6" long alumina sphere packed preheater section before entering the catalyst bed. The effluent passes through a 1/2" SS union tee to 1/4" tubing where it is diverted through a heat exchanger and a drain pot to the analytical system.

Five separately wired one-inch band heaters supply heat to each reactor. The controlling thermocouples are placed between the heaters and the reactor skin. These heaters are controlled by three individual zone controllers. The zones consisted of the preheater, hot-spot zone and the remaining catalyst bed. The reactors are insulated with one (1) inch of fiberglass Temp-Mat and two (2) inches of fiberglass pipe insulation (Microlok 650-AP).

4.1.2 Experimental Procedures

The experimental program was modified from the contract work statement during the first few months of the program in two ways. The first modification being the dilution of the feed gas with four (4) parts N_2 in order to lower the reactable CO_x concentration to 4%. This allows for improved temperature control of the highly exothermic methanation reaction. The composition of the feed gas in terms of C-H-O values is: 14.8% C - 76.0% H- 9.2% O. Operating the reactors at 1000 psig total pressure is thermodynamically equivalent to 200 psig for comparison of the mixture composition point with the carbon formation isotherms shown in Figures 8 and 9. In any event, the isotherms are relatively insensitive to pressure at pressures greater than 100 psig. Thermodynamically, this feed gas composition is slightly outside the graphite formation region.

The second contract modification involved the catalyst regeneration studies. Rather than performing a single regeneration after 1200 hours on-stream, a series of regenerations after each 300 hours of a 1200 hour scan were carried out. Regenerating in this manner will accelerate the aging effects that the regeneration cycles have on the catalyst.

The catalysts used for the duration of this experimental test program are listed in Table 2. These were chosen on the basis of nickel concentration (35-60%). These catalysts were diluted with inert alumina spheres (RHODIA SCS-9 2/4 mm), to a ratio of 1 catalyst to 1.5 inert V/V, in order to provide better hot-spot temperature control. The catalysts were activated by treating with H_2 in order to reduce the NiO to the active Ni form. The diluted catalysts were charged into the reactor baskets and placed inside the reactor. The system was then purged with N_2 at a flow of 40 liters/hour to flush it free of oxygen. Once the system was thoroughly purged, (≈ 10 min), the heaters were turned on and the reactor temperatures were controlled at $200^{\circ}F$. When the system stabilized at this temperature, the N_2 purge was turned off. The system was then purged with H_2 at a flow of 100 liters/hour. The reactors were kept at $200^{\circ}F$ for 1 hour after the start of the H_2 purge. The temperature was increased at a rate of $100^{\circ}F$ per hour to ultimately obtain a minimum

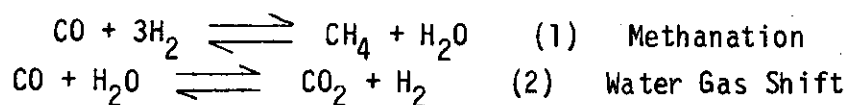
catalyst bed temperature of 600°F while keeping the hot spot below 850°F. At these final conditions, the catalyst would be fully reduced in 18 hours.

At the termination of the reduction, the system was flushed with N₂ and brought to run pressure (1000 psig) and temperature (900°F). At this time, the shifted methanation feed gas was slowly fed to the reactors at the rate of 400 liters/hour, which gave the desired VHSV of 10,000 hr⁻¹.

When the desired feed gas flow rate was obtained, the run was started. The feed gas and the reactor effluents were sampled automatically in the sequence - Feed, Effluent 1, Effluent 2, Effluent 3, Effluent 4 and Effluent 5. This sequence allowed every effluent to be sampled and analyzed at a rate of one time every two hours.

Typical GC chromatograms of the standard gas, feed gas and the reactor effluents are shown in Figures 10 through 16, respectively.

The theoretical product gas equilibrium composition was calculated (see Table 1) for comparison purposes with the effluent gas composition. The equilibrium composition was obtained by solving the equilibria relationships of reactions (1) and (2) simultaneously.



A comparison between the actual and theoretical equilibrium compositions of the effluent gases showed that all are within experimental error of the theoretical 99% CO conversion.

Also completed during the course of this project was a catalyst regeneration study using a single catalyst (UCI-CI50-4-03) throughout the test.

If air is passed over a coked catalyst hot enough to initiate combustion, a hot spot will develop due to the burning gases. As the coke is burned, the hot spot will move down the catalyst bed as a discrete layer. By

limiting the rate of oxygen supplied to the reactor, it is possible to control the catalyst temperature within a desired limit to a temperature runaway and permanent catalyst damage.

There are several techniques which can be employed to moderate the hot spot and decrease the chances of catalyst damage. One common method, and the one utilized in this study, is to reduce the O_2 concentration in the incoming gases to about 2%. This tends to thicken the hot spot and greatly reduces the peak temperature. The inert gases also aid in removing the heat of reaction. If desired, the overall rate of burning can be increased by recirculating the gases and increasing the pressure to 2 to 10 atmospheres. For this study the following regeneration procedure was used.

Fresh UCI-CI50-4-03 catalyst was loaded into each reactor and reduced in the usual way. The system was put on-stream for 300 hours and then shut down. The catalyst was unloaded and a representative sample was taken. The coked catalyst was then reloaded into the reactors. With a helium purge, the system was brought to 250°F at atmospheric pressure. Oxygen was then bled into the helium stream at the 1 to 2 percent level in order to burn off the deposited carbon under controlled conditions. The temperature was increased slowly in order to maintain a maximum hot spot somewhat lower than the nominal reaction temperature of 900°F. The catalyst bed was held at these conditions for 16 hours. The effluent gases were sampled automatically every half hour and analyzed for CO_2 and O_2 .

A sample of the regenerated catalyst was taken for total analysis. Its appearance was similar to the fresh catalyst in color but contained cracks throughout.

The regenerated catalyst was reloaded into the reactors and re-reduced with H_2 in the standard manner. On completion of the reduction, the system was flushed with N_2 and pressurized. Feed gas flow was started and the second 300-hour cycle of the regeneration test began.

This cycling was continued until the catalyst had logged a total of 1200 hours at methanation conditions. This gave a total of four 300 hour cycles and three controlled oxidative regeneration cycles.

4.1.3 Experimental Results and Discussions

All of the planned test scans were completed during the course of this work. Each scan will be presented briefly below in terms of the actual running of the experiment and the individual catalysts. The result of each of these scans will then be discussed.

The first test completed was the 100 hour scan without steam injection. This proceeded with some minor mechanical difficulties. After initial startup of the unit, only Reactor 1 was yielding acceptable results, i.e., 98+% CO conversion. The composition of the effluent from Reactors 2 through 4 was virtually unchanged from the feed gas, while the effluent from Reactor 5 showed about 60% conversion of CO. These zero and low conversion values were suspected to be due to gas leakage through a ΔP gauge, allowing the feed to completely (partly in the case of Reactor 5) by-pass the catalyst bed. This was remedied by capping off the reactor ΔP gauge. After this modification and re-reduction of the catalyst, the gas analysis was indicating essentially 100% CO conversion for all of the reactor effluents.

The CO conversion in all reactors remained virtually constant throughout the entire run. The slight differences in CO concentration from sample to sample are attributed to the statistical variations in the analytical system. The lower CO conversion obtained in Reactor 1 (98% opposed to 100%) was due to a slight gas leakage across the reactor ΔP gauge. This problem was corrected when the run terminated.

The temperature profiles for the 100 hour scan without steam are presented in Figures 17 through 21. These profiles show that over the 100 hour period, the activity of the catalysts remained unaffected by carbon deposition. This is apparent since the hot spot (main reaction zone) did not travel down the catalyst bed during the run as it would if catalyst

activity decreased due to coke accumulation on its surface. In all cases, the hot spot measured 1 to 2 inches into the catalyst bed and remained there for the entire duration of the run.

Figures 22 through 26 show the variation of component concentration versus time on stream for the five 100 hours scans. As seen in Figure 22 (Reactor 1), the CO concentration never decreased to less than 0.06 mole percent. This was due to a slight gas leakage through the reactor ΔP gauge allowing unreacted feed gas to be mixed with the effluent gas causing an increase in the CO concentration. This problem was rectified before proceeding to other tests. All of the CO concentrations are virtually 0% indicating essentially 100% CO conversion. The small amounts of CO present during the early portion of the tests are due to residual CO within the system.

The concentration of CH_4 , H_2 and CO_2 , as depicted in Figures 22 through 26, is virtually constant. The minor fluctuations are due to statistical variations within the analytical systems.

For the second five tests (300 hour without steam), fresh batches of catalyst were loaded into each reactor. During the catalyst reduction, two temperature controllers failed, causing full power to be supplied to the heaters of one reactor. When the problem was discovered, the catalyst bed had been heated to $750^{\circ}C$ ($1382^{\circ}F$) which is well above the recommended reduction temperature of $850^{\circ}F$ for the catalysts.

At this point, it was decided to recheck each of the individual controllers and heaters of the entire reactor system. Several heaters were found to be faulty and were replaced. In addition, the controlling thermocouples were repositioned around the reactor skin to enable better control of the temperature profile. The reactors were reinsulated with one (1) inch of fiberglass temp-mat and two (2) inches of fiberglass pipe insulation (Micro Lok 650-AP).

The reactors were then heated to reduction temperature ($600^{\circ}F$ min.) and the reduction continued. After the reduction was completed and all five (5) reactors were put on-stream, it was found that the over-heated

catalyst yielded only 66% CO conversion while the other four (4) catalysts were yielding 99 to 100% CO conversion. This overheated batch of catalyst was dumped from the reactor, and a fresh batch was loaded and reduced. On restarting, the fresh batch of catalyst yielded 99 to 100% CO conversion. It should be noted that during the early part of the runs, the temperature controllers are adjusted in order to fine tune the temperature profiles. This accounts for the differences between the earliest profiles and those taken later in the run.

The temperature profiles for the 300-hour scan without steam injection are shown in Figures 27 through 31. A hot spot is evident, but due to catalyst dilution and the new controlling thermocouples positioning, a quasi-isothermal catalyst bed was obtainable. The CO conversion over four of the five catalysts was 99 to 100% as indicated by the reactor effluent gas compositions shown in Figures 32 through 35. The conversion level for the fifth catalyst (Harshaw Ni-0104) was only 97% (Figure 36).

The temperature profiles for the third test scan (100 hour time test with 15% steam injection) are shown in Figures 37 through 41. The CO conversion over each of the five catalysts was 99 to 100 percent. This is indicated by the reactor effluent gas compositions shown in Figures 42 through 46. Temperature profiles for the fourth test scan (300-hour time test with 15% steam injection) are shown in Figures 47 through 51. The CO conversion during each of these tests are also 99 to 100 percent as depicted by the reactor effluent gas compositions in Figures 52 through 56.

In addition, as the results in Figure 52 show, (300-hour time test with 15% steam - United Catalyst Inc., - G87-S) instances occurred during which the concentrations of the CO_2 and H_2 rapidly decreased, while that of CH_4 increased. This was due to two (2) short-term water pump failures (at 50 and 125 hours) during the test. With the loss of co-fed water, the water gas shift reaction equilibrium shifts to $(\text{CO} + \text{H}_2\text{O} \rightleftharpoons \text{CO}_2 + \text{H}_2)$ the left. That is, there is a decrease in CO_2 and H_2 concentrations and an increase in CO concentration. However, at the same time, because of the lower water concentration, the methanation reaction $(\text{CO} + 3\text{H}_2 \rightleftharpoons \text{CH}_4 + \text{H}_2\text{O})$ shifts to the right, with a resultant increase in CH_4 concentration.

The temperature profiles for the 600-hour time test without steam injection are shown in Figures 57 through 61. The CO conversion over each of the five catalysts was between 98 and 100 percent as is depicted in Figures 62 through 66. The 600-hour time test with 15% steam injection temperature profiles are presented in Figures 67 through 71. The concentration versus time curves are shown in Figures 72 through 76. These indicate that in all cases, CO was at least 98% converted.

Figures 57 through 61 and Figures 67 through 71 show a maximum hot spot temperature of 485-495°C. The temperature profiles along the catalyst beds are very stable with little downward migration. This suggests that after 600 hours, the catalyst activity has not decreased significantly.

The 1200-hour time test without steam injection temperature profiles are shown in Figures 77 through 81. The CO conversion over each of the five catalysts was between 98 and 100 percent as depicted in Figures 82 through 86. Early in this test run, the product gas analysis from Reactor 4 (Harshaw Ni-3210) began to show a slowly increasing CO level. Initially, this was thought to be due to a gradual loss in catalyst activity, possibly as a result of carbon deposition. However, it was later recognized that there was a minor malfunction in the analytical system. After making the necessary adjustments, the measured product gas CO level again fell to the expected 0.01 v/o level.

The 1200 hour - 15% steam scan temperature profiles are shown in Figures 87 through 91. These profiles indicate a hot spot temperature of 485-500°C. The profile along the catalyst bed is very stable with no forward movement of the hot spot. The CO conversion over each of the catalysts was 99 to 100% as shown in Figures 92 through 96. It can be seen from these figures that there were instances during which the concentrations of CO₂ and H₂ decreased, while that of CH₄ increased. This was due to several intermittent water pump failures. As mentioned earlier, the loss of co-fed water causes the water gas shift reaction equilibrium ($\text{CO} + \text{H}_2\text{O} \rightleftharpoons \text{CO}_2 + \text{H}_2$) to shift to the left,

thereby decreasing the concentrations of CO_2 and H_2 and increasing the CO concentration. Simultaneously, due to the lower H_2O concentration, the equilibrium of the methanation reaction ($\text{CO} + 3\text{H}_2 \rightleftharpoons \text{CH}_4 + \text{H}_2\text{O}$) shifts to the right. This shift increases the CH_4 concentration.

Temperature profiles for each of the four regeneration cycle scans using the UCI-C150-4-03 catalyst are presented in Figures 97 through 100. As seen, the hot spot was always located in the first quarter of the catalyst bed. This indicates that the active catalyst can be successfully oxidized and re-reduced to its previous high activity. This is supported in the component concentration curves shown in Figures 101 through 104, which indicate that the CO conversion was 98 to 100% complete throughout the entire test. Figure 105 depicts the effect that a controlled in-situ oxidative regeneration has on the crush strength of the catalyst. Initially, the catalyst loses a significant amount of strength, from 7.75 kg to 1.3 kg during the first 300 hours. After three regenerations and 900 additional hours on-stream, the crush strength decreased to 0.6 kg. This is compared in Figure 106 to the crush strength of the same catalyst after 1200 hours of continuous running under similar conditions without any regeneration. This indicates that the in-situ oxidation of the surface carbon from the catalyst does not reduce the strength of the catalyst any more than normal operation. From a strength point of view, this would seem to be a potential method of increasing effective catalyst life in a reactor.

The following synopsis pertains to the individual tested catalysts. A general discussion will follow. The pertinent catalyst results are presented in summary in Tables 6 through 11.

Harshaw Ni-3210

As shown in Figure 107 and Table 6, the nickel crystallite size increased in the absence of steam at a gradual rate from its initial 65 \AA to 85 \AA . When steam was injected, the nickel crystals grew to 127 \AA . With this increase in Ni crystallite size a decrease in the nickel surface area is

expected. This is verified in Figure 108 and Table 7 which show the decrease in nickel surface area from $74 \text{ m}^2/\text{g}$ for the fresh catalyst to $54.3 \text{ m}^2/\text{g}$ without steam and $37.8 \text{ m}^2/\text{g}$ with steam injection. Also seen (Figure 109 and Table 8) is the overall decrease in catalyst surface area from the initial $159.0 \text{ m}^2/\text{g}$ to $74.0 \text{ m}^2/\text{g}$ and $49.7 \text{ m}^2/\text{g}$ without and with steam injection, respectively. The mercury pore volume (Figure 110 and Table 9) showed an increase from 0.14 cc/g to 0.27 cc/g in the absence of steam and to 0.23 cc/g in the presence of steam. An increase in carbon content is shown in Figure 111 and Table 10. The carbon content seems to stabilize near the 300-hour mark, indicating that about 300 hours are required for the carbon to reach equilibrium on the catalyst surface. At this point, the rate of carbon formation is equal to the rate of carbon utilization to form methane. The carbon present as graphite is due to the organic binder utilized during pelletization of the catalyst.

Figure 112 illustrates the change in catalyst strength with time. It is noted that the strength of the catalyst remained essentially constant throughout the test. The presence of water increased the crush strength. This seems to be due to a morphological change in the CaCO_3 support material. As time progressed, the crystallite size of the CaCO_3 increased. This increase was more pronounced in the presence of steam indicating that an increase in support crystallite size may strengthen the support material.

UCI-G87-S

The nickel crystallite size (Figure 113; Table 6) increased slightly when steam was not injected from 100 \AA to 320 \AA . When steam was injected, the growth of the crystals were greatly accelerated to a final size of 1322 \AA . The catalyst surface area (Figure 114; Table 8) decreased rapidly from $72 \text{ m}^2/\text{g}$ to $30 \text{ m}^2/\text{g}$ in 100 hours and then stabilized at $40 \text{ m}^2/\text{g}$ for the remaining time. In the presence of steam, the initial rapid decrease followed the same path to $30 \text{ m}^2/\text{g}$ but continued to decrease gradually to $15 \text{ m}^2/\text{g}$ where it stabilized. The surface area of the

nickel (Figure 115; Table 7) decreased from 20 m²/g to 15 m²/g without steam injection and to 5 m²/g with steam injection. The pore volume (Figure 116; Table 9) both with and without steam injection decreased from 0.49 to 0.58 cc/g during the first 100 hours. It stabilized at this point when steam was not injected but continued to decrease gradually to 0.38 cc/g when steam was injected.

The carbon content (Figure 117; Table 10) increased from the initial 0.2 to 1.2 wt% in 100 hours and stabilized at about 1.3 wt% when steam was not injected. With steam injection, the initial increase in carbon was to 1.7 wt% in 100 hours with a gradual decrease in 1.2 wt% at the end of the run. The crush strength (Figure 118) decreased significantly during the first 100 hours from 10.8 kg to 4.3 and 4.7 kg for the scans with and without steam injection, respectively. These continued to decrease with time on-stream to 1.5 kg and 3.3 kg at the end of the run with and without steam, respectively.

Harshaw Ni-0104

The nickel crystallite size (Figure 119; Table 6) increased slightly from 60 Å to 100 Å without steam injection and to 120 Å with steam injection. The overall catalyst surface area (Figure 120; Table 8) decreased gradually from 140 m²/g to 55 m²/g and 52 m²/g in the absence and presence of steam, respectively. The nickel surface area (Figure 121; Table 7) increased from 45 m²/g to 58 m²/g in 100 hours and then stabilized at 48 m²/g when steam was not injected. With steam injected, the surface area of the nickel increased sharply to 78 m²/g in the first 100 hours and then decreased and stabilized at 40 m²/g for the remainder of the test. The pore volume (Figure 122; Table 9) showed only a slight increase from 0.14 cc/g to 0.2 cc/g without steam and 0.16 cc/g with steam. When steam was not injected, the carbon content (Figure 123; Table 10) increased from 4.1 to 5.5 wt%. With steam, the carbon increased to 5.4 wt% after 300 hours and then stabilized at 4.6 wt% for the remainder of the test. The crush strength (Figure 124) decreased slightly from 4.7 kg to 3.75 kg without steam and to 2.9 kg with steam injection.

UCI-C150-4-03

The nickel crystallite size (Figure 125; Table 6) of this catalyst increased from the initial 30 Å to 140 Å when steam was not injected. With steam, the crystals increased to 240 Å. The surface area (Figure 126; Table 8) decreased rapidly in 100 hours from 175 m²/g to 55 m²/g where it stabilized. When steam was injected, the surface area decreased slowly during the entire test to 35 m²/g. The nickel surface area (Figure 127; Table 7) decreased rapidly in 100 hours from 38 m²/g to 15 m²/g then increased to and stabilized at 36 m²/g for the remainder of the test. In the presence of steam, a rapid increase in nickel surface area to 55 m²/g was noted at the 300-hour point with a gradual decrease and stabilization at 20 m²/g at the test's termination. The pore volume (Figure 128; Table 9) showed a rapid increase in 100 hours from 0.2 cc/g to 0.38 cc/g and then stabilized at 0.36 cc/g. When steam was injected, the pore volume rapidly increased to 0.34 cc/g in 100 hours and stabilized itself in that area for the remainder of the run. The carbon content (Figure 129; Table 10) increased from the initial 2.5 wt% to 3.5 wt% gradually when steam was not injected. In the presence of steam, however, the overall carbon content decreased to 2.2 wt%. The crush strength (Figure 130) of the catalyst decreased rapidly from 7.7 kg to 1.2 kg at 100 hours of operation both with and without steam addition. After this initial drop, there was little change in strength. At the 1200 hour point the crush strength was 0.4 and 1.0 kg with and without steam, respectively.

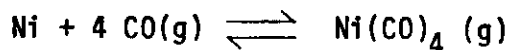
Katalco CRG-F

Without steam injection, the nickel crystallite size (Figure 131; Table 6) of this catalyst increased from the initial 20 Å to 140 Å. This increase was much greater in the presence of steam where the crystals grew to 290 Å. The catalyst's surface area (Figure 132; Table 8) decreased slowly from 135 m²/g to 70 m²/g without steam and to 35 m²/g when steam was injected. The nickel surface area (Figure 133; Table 7), however, increased from 23 m²/g to 35 m²/g in 100 hours and remained there for

the duration of the test. When steam was injected, the nickel surface area increased from the initial $23 \text{ m}^2/\text{g}$ to $55 \text{ m}^2/\text{g}$ in 100 hours and then decreased to $17 \text{ m}^2/\text{g}$ at the 1200-hour point. The pore volume (Figure 134; Table 9) was essentially constant, increasing from 0.3 cc/g to 0.35 cc/g and 0.34 cc/g with and without steam injection. The carbon content (Figure 135; Table 10) increased slightly from 2.4 to 3.7 wt% when steam was not present. When steam was injected, the carbon content showed an increase to 3.5 wt% at 300 hours but then slowly decreased and stabilized at 3.0 wt%. The crush strength (Figure 136) decreased slightly during the course of the study from 2.6 kg to 1.4 kg. In the presence of steam, the catalyst crush strength was decreased to 0.4 kg.

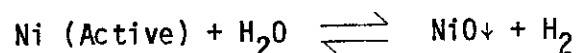
In all cases, an increase in nickel crystallite size was noted. This increase was more pronounced in the presence of steam. This may have been due to sintering of the nickel if the surface temperature of the catalyst was allowed to exceed 600°C . Since the reaction was carried out at $<500^\circ\text{C}$, it is safe to assume that very little growth was due to excessive temperature.

One possibility is the formation of $\text{Ni}(\text{CO})_4$ by the following reaction:



The product $\text{Ni}(\text{CO})_4$ molecules can leave the metal particle and diffuse through the gas phase and/or over the catalyst support. These species can then decompose to metallic Ni on either a nearby Ni particle or a Ni particle on a catalyst granule downstream. This type of growth seems unlikely for this system since the partial pressure of CO in the feed gas was kept very low.

What may be responsible for the observed nickel crystallite growth is known as steam poisoning. This involves a catalyst deactivation - activation cycle proceeding via the following reaction:



This type of catalyst poisoning (due to reduction in active Ni concentration) is a known occurrence at high steam to H_2 ratios.

In the present case, this type of catalyst deactivation would occur when a significant portion of the H_2 present in the feed gas is consumed during methane production. From a study of the temperature profiles, the bulk conversion takes place in the upper portion of the catalyst bed. With a decrease in H_2 concentration, the reaction would shift to the right. With the resultant increase in inactive NiO, the catalyst activity would decrease in the upper portion of the bed. On decreasing the catalysts' activity, the conversion of the feed gas would be reduced resulting in an increase of H_2 in the initial portion of the catalyst bed. This would tend to shift the reaction back to the left. By doing this, the inactive NiO is harshly reduced to the active Ni form. It is known that if a Ni catalyst is activated by reducing with H_2 , the resulting crystallite size of the active Ni would depend extensively on the degree of reduction severity. A reduction occurring under the nominal reaction conditions is considered to be very harsh.

Although the crystallite size of the Ni particles increased during each of the test scans, at no time did this increase affect the overall catalyst activity. In all cases and throughout each run, the conversion of CO was always 98-100% complete. These high conversions are realized due to the overall length of the catalyst bed (12 inches). Since the reaction is occurring mainly in the upper 2 to 3 inches of the bed, the remaining 9 to 10 inches is simply a catalyst reservoir functioning as a polisher to obtain the equilibrated effluent gas mixture.

The increase in pore volume is also enhanced in the presence of steam. An increase in the size of catalyst pores is usually associated with a composition change in the support material. This change may be due to the hydration of the support, usually Al_2O_3 , or a structural change from the α to γ or other form of Al_2O_3 . Any change of this type can greatly effect the pore volume.

The surface area of the catalyst and that of the nickel both decreased during each of the scans. This is expected with the increased Ni crystallite size and pore volume.

Carbon was deposited on all the catalysts under the methanation conditions studied. The amount of carbon that was determined to be on the surface of the catalysts may not be indicative of the total carbon formed but rather the bulk non-methane forming carbon. A high activity toward carbon formation was found to be associated with the catalysts with the higher Ni surface area. The incorporation of steam into the system reduced the overall carbon content. The more dilute catalysts, i.e., those of lesser Ni concentration, were more resistant to carbon formation. This is probably due to a stronger interaction of the nickel with the support material. From these findings, one can see that the rate of carbon deposition was primarily a function of the catalyst properties and not of the thermodynamics of the methanation reaction system. In spite of heavy carbon deposition, the catalytic behavior of these systems remained unaffected. The limiting condition would be the physical plugging of the catalyst bed and not catalyst deactivation. In this respect, the controlled oxidation of the carbon deposits might be a viable method of extending catalyst life.

With the formation of carbon deposits during methanation, a disintegration of catalyst pellets due to internal stresses produced by the increased concentrations of the strong carbon filaments was also expected. This was found to be true except in the case of the two Harshaw catalysts tested. The strength of these catalysts remained unchanged throughout the entire test scan.

4.1.4 Conclusions and Recommendations

- Based on observations of measured temperature profiles, the reaction hot spot is always near the top of the catalyst bed. This indicates that very short catalyst contact times are required for nearly complete conversion of CO. The remainder of the catalyst bed only serves as a catalyst reservoir. Any future work should be performed with a catalyst bed operated in the kinetic regime utilizing a differential fixed-bed reactor. This will enable swifter evaluation of the parameters suspected of influencing the deactivation of the catalyst.
- This study showed that an active catalyst can be carefully oxidized and re-reduced to obtain its original high activity. Future work should include a study to determine if a deactivated catalyst (due to carbon) can be regenerated and re-reduced to its initial high activity.
- In all but one case, a decrease in catalyst crush strength was noted. If the crush strength of the catalyst is significantly decreased during operation, it will be pulverized under its own weight causing plugging of the reactor and shutdown. Future work should include an investigation of the effects of process variables on the catalysts' crush strength.
- Future work should include a study which will concentrate on the development of a promoted nickel catalyst which would be more resistant than nickel to carbon formation under carburizing conditions.
- Deactivation may be temperature dependent, and future experiments should include a study of the temperature dependence of catalyst sintering under strong reducing conditions.